Ecological Indicators 77 (2017) 218–227

Contents lists available at ScienceDirect

Ecological Indicators

journal homepage: www.elsevier.com/locate/ecolind

Improved retrieval of Secchi depth for optically-complex waters using remote sensing data

Krista Alikas[a,*], Susanne Kratzer[b]

[a] Tartu Observatory, Department of Remote Sensing, Group of Remote Sensing of Waterbodies, Tartumaa, Tõravere, 61602, Estonia
[b] Stockholm University, Department of Ecology, Environment and Plant Sciences, Stockholm SE-106 91, Sweden

ARTICLE INFO

Article history:
Received 15 February 2016
Received in revised form 3 February 2017
Accepted 6 February 2017
Available online 25 February 2017

Keywords:
Secchi depth
ENVISAT/MERIS
Sentinel-3/OLCI
Lakes
Optically complex waters
Water framework directive
Environmental monitoring

ABSTRACT

Water transparency is one of the ecological indicators for describing water quality and the underwater light field which determines its productivity. In the European Water Framework Directive (WFD) as well as in the European Marine Strategy Framework Directive (MSFD) water transparency is used for ecological status classification of inland, coastal and open sea waters and it is regarded as an indicator for eutrophication in Baltic Sea management (HELCOM, 2007). We developed and compared different empirical and semi-analytical algorithms for lakes and coastal Nordic waters to retrieve Secchi depth (Z_{SD}) from remote sensing data (MERIS, 300 m resolution). The algorithms were developed in water bodies with high coloured dissolved organic matter absorption ($a_{CDOM}(442)$ ranging 1.7–4.0 m^{-1}), Chl *a* concentration (0.5–73 mg m^{-3}) and total suspended matter (0.7–37.5 g m^{-3}) and validated against an independent data set over inland and coastal waters (0.6 m < Z_{SD} < 14.8 m). The results indicate that for empirical algorithms, using longer wavelengths in the visible spectrum as a reference band decreases the RMSE and increases the coefficient of determination (R^2). The accuracy increased (R^2 = 0.75, RMSE = 1.33 m, n = 134) when Z_{SD} was retrieved via an empirical relationship between Z_{SD} and $K_d(490)$. The best agreement with in situ data was attained when Z_{SD} was calculated via both the diffuse and the beam attenuation coefficient (R^2 = 0.89, RMSE = 0.77 m, n = 89). The results demonstrate that transparency can be retrieved with high accuracy over various optical water types by the means of ocean color remote sensing, improving both the spatial and temporal coverage. The satellite derived Z_{SD} product could be therefore used as an additional source of information for WFD and MSFD reporting purposes.

1. Introduction

Water transparency is one of the key components describing the water quality and the productivity of natural waters. Water transparency is used for ecological status classification of coastal and open sea waters in the European Water Framework Directive (WFD, European Commission, 2000) as well as in the European Marine Strategy Framework Directive (MSFD, European Commission, 2008). Inclusion of satellite remote sensing products for monitoring water transparency would substantially increase the description of spatial, seasonal and long-term changes.

The biological (e.g. phytoplankton photosynthesis), physical (e.g. heat transfer, sediment resuspension) and chemical (e.g. nutrient cycling) processes taking place in the water column are dependent on the underwater light field. Before the availability of radiometers, the underwater light field was estimated only by the visual observations of the Secchi disk. Historical records of the Secchi depth (Z_{SD}) are some of the earliest water quality measurements available, dating back to the nineteenth century (see Aas et al., 2014 for a thorough review). This parameter is easily understandable for the public.

The Secchi depth is influenced by the three main optical components: chlorophyll-*a* (Chl-*a*), coloured dissolved organic matter (CDOM), and total suspended matter (TSM). In the Baltic Sea, CDOM contributes substantially to the variability in Secchi depth, and also TSM in coastal waters (Håkanson et al., 2004). As Secchi depth is an indicator for eutrophication in Baltic Sea management (HELCOM, 2007), high concentrations of TSM and CDOM may also affect the eutrophication assessments.

Due to its simple and universal method, the Secchi disk is still currently used for measuring water transparency and estimating the order of magnitude of optical substances in water. Additionally, the attenuation of light can be described by optical measurements estimating the vertical diffuse attenuation coefficient (K_d, m^{-1}) and

* Corresponding author.
E-mail addresses: alikas@to.ee (K. Alikas), Susanne.Kratzer@su.se (S. Kratzer).

http://dx.doi.org/10.1016/j.ecolind.2017.02.007
1470-160X/

the beam attenuation coefficient (c, m^{-1}) (Kirk, 1994). Both parameters are strongly wavelength (λ) dependent. Tyler (1968) showed that vertical visibility, i.e. Z_{SD}, is closely related to the inverse of the sum of $K_d + c$.

Based on the empirical observations, Poole and Atkins (1929) showed an approximately inverse relationship between the diffuse attenuation coefficient K_d and Z_{SD} in marine waters. Empirical and semi-analytical algorithms have also been used to estimate Z_{SD} from remote sensing data. Kratzer et al. (2003) found a good linear regression ($R^2 = 0.72$) between K_d(PAR) and Z_{SD}, based on the data from coastal waters of the NW Baltic Sea. Over coastal and inland waters, the amount of absorbing and scattering substances is higher and therefore the inversion from Secchi depth to K_d is more complex than in optical case 1 waters, i.e. in waters were the optical properties are dominated by water and phytoplankton. The regression is commonly described as a power function over more turbid waters (Chen et al., 2007a). Austin and Petzold (1981) developed an empirical algorithm based on the blue to green radiance ratio for K_d(490) for case 1 waters. This approach was tuned to regional conditions by various studies (e.g. Doron et al., 2007; Kratzer et al., 2008; Wang et al., 2009; Alikas et al., 2015a) which showed that for optically-complex waters the reference band in the ratio should be in the red part of the spectrum rather than in the green which is only appropriate for case 1 waters.

Tyler (1968) showed that in theory, the Z_{SD} is related to the inverse value of the total diffuse attenuation coefficients, $K_d(\lambda)$, and the beam attenuation coefficient $c(\lambda)$. Many studies derived the relationship between the Z_{SD} and $K_d(\lambda) + c(\lambda)$ on the basis of empirical data from coastal (Tyler 1968; Holmes 1970; Aas et al., 2014) and inland waters (Vant and Davies-Colley, 1984; Davies-Colley and Vant, 1988; Kallio 2006). The method has been also applied directly to remote sensing data (Doron et al., 2011), where instead of using predefined relationship between Z_{SD} and $K_d(\lambda) + c(\lambda)$, the band at 490 nm was used to estimate the so-called photopic contrast reduction for each match-up pixel separately. Lee et al. (2015) have updated the underwater visibility theory introduced by Tyler (1968) and developed a new theoretical model which relies only on the diffuse attenuation coefficient at a given wavelength (443, 488, 532, 555, 665 nm), corresponding to the maximum transparency.

In this paper, three approaches were compared for the retrieval of Z_{SD} values by means of MERIS-derived products. Firstly, varying sets of band ratio algorithms were tested using wavelengths corresponding to the MERIS bands (490, 560, 620, 660, 680, 709 nm). Secondly, the relationship between the diffuse attenuation coefficient, $K_d(490)$ and Z_{SD} was analyzed and applied on previously derived $K_d(490)$ values, which served as input for the algorithm. Thirdly, the theoretical relationship between Z_{SD} and the sum of $K_d(\lambda)$ and the beam attenuation coefficient $c(\lambda)$ was applied.

The aim of this study is to develop and assess various algorithms in order to find the most suitable algorithm for deriving Secchi depth for optically-complex waters from remote sensing data. The data used in the study comprised both Baltic Sea as well as Nordic inland waters. For this study, data from MERIS sensor was used since it has the highest radiometric, spectral and spatial resolutions compared to other common Ocean Colour sensors (MODIS, SeaWiFS), and therefore is also capable of monitoring coastal and inland waters. Additionally, MERIS is a precursor for the new water quality sensor OLCI on-board Sentinel-3 which was launched on 16th February in 2016. Satellite data used for the validation purposes were processed with three different sets of atmospheric correction and bio-optical modules in order to document the robustness of the algorithms. The algorithms were directly validated using in situ measurements of Secchi depth over both coastal and inland waters.

2. Materials and methods

2.1. Description of the algorithms

Three different approaches were tested to estimate the Secchi depth (Fig. 1). Algorithms were calibrated with the bio-optical datasets measured from coastal (Kratzer et al., 2008; Paavel et al., 2011) and inland (SUVI dataset, Arst et al., 2008) waters.

2.1.1. Secchi depth via remote sensing reflectance, Z_{SD} via R_{rs}

In the first approach (Fig. 1), an empirical band ratio algorithm developed originally after Austin and Petzold (1981) for estimating K_d(490) from blue to green water-leaving radiances was modified by Kratzer et al. (2008) to estimate Secchi depth (Eq. (1)) for remote sensing applications. The empirical Z_{SD} algorithm was developed based on in situ measured data where the log-transformed Secchi readings were plotted against different log-transformed band ratios:

$$Z_{SD} = A\left[\frac{R_{rs}(\lambda_1)}{R_{rs}(\lambda_2)}\right]^B, \quad (1)$$

where A and B are coefficients derived by linear regression analyses and R_{rs} is the reflectance at different MERIS wavelengths.

2.1.2. Secchi depth via the diffuse attenuation coefficient, $K_d(490)$

In the second approach, the Secchi depth readings were plotted against simultaneously measured $K_d(490)$ values and subsequently the conversion factors A and B were derived:

$$Z_{SD} = A[K_d(490)]^B \quad (2)$$

2.1.3. Secchi depth via the sum of the diffuse and the beam attenuation, $K_d(\lambda) + c(\lambda)$

In the third approach, Secchi depth is expressed by the photopic contrast reduction for a vertical path of sight in a homogeneous medium by Tyler (1968):

$$Z_{SD} = \frac{\ln\left(\frac{C_0}{C_{min}}\right)}{K_d(PAR) + c(PAR)}, \quad (3)$$

where $K_d(PAR)$ and $c(PAR)$ are the vertical diffuse attenuation and beam attenuation coefficients over the photosynthetically active radiation (PAR), C_{min} is the minimum apparent contrast perceivable by the human eye, C_0 is the inherent contrast between the Secchi disk depth and the background water reflectance, and is calculated as:

$$C_0 = \frac{R_{rs}(Secchi) - R_{rs}(water)}{R_{rs}(water)}, \quad (4)$$

where the R_{rs}(Secchi) corresponds to the reflectance of the Secchi disk and R_{rs}(water) is the reflectance of the water, taking the sensitivity of the human eye into account (Mobley, 1994).

In this study, the coupling constant $\ln\left(\frac{C_0}{C_{min}}\right)$ was calculated in three different ways to distinguish a target (Secchi disk) from its background (water). First, we used in situ datasets to calculate average coupling constant for inland and coastal waters. Second, similarly to Doron et al. (2011), we used the reflectance value at single wavelength where light penetrates deepest to better reproduce the photopic contract reduction:

$$\ln\left(\frac{C_0}{C_{min}}\right) = \ln\frac{\frac{R_{rs}(Secchi) - R_{rs}(\lambda)}{R_{rs}(\lambda)}}{C_{min}}, \quad (5)$$

where $R_{rs}(\lambda)$ is the band either at 490 nm, 510 nm, or 560 nm.

Third, instead of a single band in the coupling constant we used reflectance value at all visible MERIS bands taking the sensitivity of the human eye into account (Mobley, 1994).

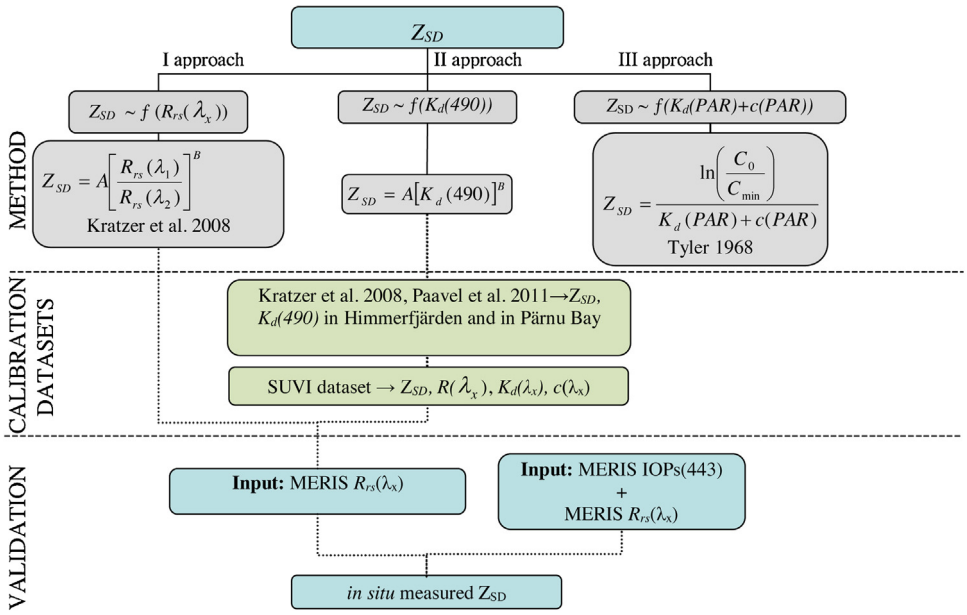

Fig. 1. Development and validation of Secchi depth algorithms.

2.2. Dataset for the development of the algorithms

For the approaches I and III, a dataset collected in 14 Estonian and 7 Finnish lakes (Arst et al., 2008) was used to develop a Z_{SD} algorithm. These lakes cover a wide range of Z_{SD} (Table 1) and thus also a wide range of the other optical in-water components a_{CDOM} ($0.2 < a_{CDOM}(442)\,m^{-1} < 6.7$), Chl a ($0.5 <$ Chl a$(mg\,m^{-3}) < 73$) and TSM ($0.7 < C_{TSM}(g\,m^{-3}) < 37.5$). The dataset consisted of 63 simultaneous Secchi depth, $K_d(\lambda)$, $c(\lambda)$ and irradiance reflectance measurements ($R(\lambda)$) below the surface measured with a Li-COR instrument.

For the approach II, a dataset representing Baltic Sea coastal areas (Himmerfjärden bay in the NW Baltic proper on the Swedish coast, and Pärnu Bay in the NE Baltic proper on the Estonian coast) was included to analyze the conversion factors between Z_{SD} and $K_d(490)$. For Himmerfjärden bay, in situ data was measured during 2000–2002 (Kratzer et al., 2008) and 2008 (Kratzer and Vinterhav, 2010). For Pärnu Bay, Z_{SD} and $K_d(490)$ values were measured in 2006 and 2007 (Paavel et al., 2011).

2.3. Datasets for the validation

The validation was performed over varying types of optical case 2 waters (i.e. with varying contributions of Chl a and TSM concentration and CDOM absorption): two coastal sites and five lakes (Table 1). The Z_{SD} measurements measured in situ were from both the Estonian (Peipsi, Võrtsjärv; Secchi disk diameter 30 cm) and Swedish (Mälaren, Vänern, Vättern; Secchi disk diameter 25 cm) national lake monitoring programs. The Z_{SD} readings from the coastal sites (Secchi disk diameter 30 cm in both cases, whereas water telescope was used in Himmerfjärden bay) were collected during the cruises described in the previous section (see dataset for the development of the algorithms) which differ from the measurements used for algorithm development.

2.4. MERIS data used for the validation

The algorithms were validated using coincident sets of MERIS reflectance and IOP (inherent optical properties) data and Z_{SD} measured in situ. Altogether 165 match-ups were compiled from 104 MERIS Level 1b (IPF 6.04) full resolution images. L1b images were first pre-processed with a Radiometry processor (Bourg et al., 2008) to remove smile-effects and then with the Improved Contrast between Ocean and Land (ICOL v.2.7.4., Santer and Zagolski, 2008) to remove possible adjacency effects from land. For level 2 processing, the neural networks and bio-optical models of three different processors were used: 1) MERIS standard (MEGS 6.01, ESA, 2011); 2) the case-2 water algorithm from Free University of Berlin (FUB, WeW, Schroeder et al., 2007); 3) the Case-2 regional algorithm (C2R, version 1.5.3, developed by Doerffer and Schiller, 2008). The image processing was done using BEAM 4.9 (Brockmann Consult 2010) and the ODESA CFI software.

For the validation, classification flags were first applied on each match-up pixel to exclude land and cloud pixels. Secondly, various confidence and science flags or combination of them were applied in order to find the most effective approach to eliminate invalid pixels. For MEGS the confidence flag PCD1_13 was applied which tests if the 13 water-leaving reflectances are all positive rather than negative. For C2R, pixels were checked for the atmospheric correction flags (agc_flags), indicating if the atmospheric correction was out of range. For the FUB WeW processor, all pixels were excluded for which flags indicated atmospheric correction failure in the input or output data.

Depending on the approach, the inputs used for the different algorithms were the MERIS-derived R_{rs} values at various wavelengths or the IOPs (Fig. 1). Marine reflectances from MEGS and water leaving reflectances from FUB and C2R were taken directly from level 2 products from the respective bands. For the II approach $K_d(490)$ was first calculated according to Alikas et al. (2015a) using MERIS R_{rs} bands at 490, 560 and 709 nm. For the approach III, the IOPs were taken from the level 2 products of MEGS and C2R which were scaled to 490 nm based on the regional conversion factors taken from Kratzer (2000) and described in Alikas et al. (2015a).

2.5. Accuracy assessment

Model performance was estimated combined by the coefficient of determination (R^2), the number of match-ups (n), the root mean squared error (RMSE), the relative root mean squared error (RRMSE) and the mean normalized bias (MNB):

$$RMSE = \sqrt{\frac{1}{n}\sum_{i=1}^{n}\left(X_{insitu,i} - X_{Model,i}\right)^2}, \quad (6)$$

Table 1
Description of data used for algorithm development (*) and for the validation (**).

	Chl a ($mg\,m^{-3}$)	TSM ($g\,m^{-3}$)	a_{CDOM} (443 nm)	Secchi depth m
Lakes*	0.5–73	0.7–37.5	0.2–6.7	0.2–15.0
Himmerfjärden*,**	1.2–11.6	0.5–4.8	0.3–0.8	1.9–7.5
Pärnu Bay*,**	0.7–10.7	5.0–24.3	0.6–3.7	0.6–4.3
Mälaren**	1.2–98.2	1.4–11.2	1.2–7.7	0.5–4.2
Peipsi**	2.7–122	1.3–61.3	1.2–7	0.4–3.6
Vänern**	1.2–9.5	0.5–0.7	0.5–2.8	1.2–7.2
Vättern**	0.6–9.8	0.4–2.3	0.07–1.2	8.5–16.2
Võrtsjärv**	3.4–72.2	1.6–52.7	1.9–8.9	0.2–2.6

Table 2
Derived parameters and respective coefficient of determination for various wavelengths on estimating Secchi depth. The parameters are shown in the table as follows: $SD = \left(\frac{R(\lambda)}{R(\lambda)}\right)^{A} \cdot B$.

	A	B	R^2
$R(490)/R(620)$	1.16	4.19	0.66
$R(490)/R(660)$	0.89	2.95	0.66
$R(490)/R(709)$	0.70	2.14	0.73
$R(560)/R(709)$	0.79	1.12	0.66

$$RRMSE = \sqrt{\frac{RMSE}{\frac{1}{n}\sum_{i=1}^{n} X_{insitu,i}}} \cdot 100, \quad (7)$$

$$.MNB = \frac{1}{n}\sum_{1}^{n}\left(\frac{X_{Model,i} - X_{insitu,i}}{X_{insitu,i}}\right) \cdot 100, \quad (8)$$

where n is the total number of match-ups, $X_{insitu,i}$ is the observed in situ value and $X_{Model,i}$ is the estimated value.

3. Results

3.1. Tuning the secchi depth algorithms to regional conditions

3.1.1. Secchi depth via remote sensing reflectance, Z_{SD} via R_{rs}

Various band ratios, corresponding to MERIS bands, were tested to derive a Secchi depth algorithm based on the SUVI dataset. Since the below surface irradiance reflectance R(λ) and above surface remote sensing reflectance $R_{rs}(\lambda)$ are strongly correlated (Vertucci and Likens, 1989), the band ratio algorithms were derived on the irradiance reflectance values R(λ) from the SUVI dataset and applied to MERIS derived $R_{rs}(\lambda)$ values. The results from the band ratios explaining most of the variance in Secchi are shown in Table 2.

The ratio $R(490)/R(709)$ described most of the variance ($R^2 = 0.73$), resulting in the following algorithms:

$$SD = \left(\frac{R(490)}{R(709)}\right)^{0.697} \cdot 2.137, \quad (9)$$

The lowest correlation ($R^2 = 0.30$) was obtained with the $R(490)/R(560)$ ratio, which is the ratio commonly used to map transparency over clear ocean waters (Mueller, 2000).

3.1.2. Secchi depth via the diffuse attenuation coefficient, $K_d(490)$

Regression analyses were performed based on the simultaneously measured $K_d(490)$ and Z_{SD} values in the Baltic Sea and in inland water datasets (Fig. 2).

The highest correlation ($R^2 = 0.84$) was obtained when considering datasets measured over the Baltic Sea coastal areas together. Data over clearer coastal waters, Himmerfjärden, complemented well the much more turbid dataset from Pärnu Bay. There was more scatter in the lake dataset since it represented oligotrophic to eutrophic lakes with various transparencies, and the data thus spanned over a wider range with $R^2 = 0.81$. In general the measurements from the SUVI dataset fitted well with the data measured over the coastal areas. The regression lines in case of both coastal and inland water datasets were almost identical in case of very low ($Z_{SD} < 1.5$ m) and high ($Z_{SD} > 10$ m) transparency values.

3.1.3. Secchi depth via the sum of the diffuse and the beam attenuation, $K_d(\lambda) + c(\lambda)$

Based on the SUVI dataset, the algorithm by Tyler (1968) (Eq. (3)) was tuned to local conditions. Using the assumption for the Secchi disk reflectance to be 82% and c_{min} to be 0.0066 after Tyler (1968), the actual calculated values ranged between 6.96 and 10.36, with an average of 8.35.

Therefore, Eq. (3) was applied by using a value of 8.35 for the coupling constant, and also by calculating the coupling constant for each match-up pixel separately either by a single band (490, 510, 560 nm) or using the full spectrum in the visible domain.

Secondly, similarly to Doron et al. (2007), a very strong correlation ($R^2 = 0.99$) was found between $K_d(PAR) + c(PAR)$ and $K_d(490) + c(490)$ based on the SUVI dataset:

$$K_d(PAR) + c(PAR) = -0.0001x^2 + 0.7809x + 0.4026, \quad (10)$$

where x stands for $K_d(490) + c(490)$. This allowed to estimate Z_{SD} (Eq. (3)) by calculating the $K_d(490)$ and $c(490)$ first (the sum of total absorption and total scatter at 490 nm) from MERIS data after Alikas et al. (2015a), and then interpolating the value for the PAR region.

3.2. Validation of the Secchi depth algorithms

Z_{SD} was derived most accurately from the products of MEGS over the coastal areas (Fig. 3). The validation results from FUB and C2R had lower correlation coefficients and higher root mean square errors. Removing the flagged data had most effect on the results of MEGS products.

According to the higher uncertainty in case of the derived Z_{SD} from the FUB and C2R products (Fig. 3), the validation over all sites (lakes included) was subsequently performed only on the MEGS products. Validation results over Himmerfjärden showed that among band ratio algorithms, the model based on 490/709 could estimate Z_{SD} with the lowest error ($R^2 = 0.11$, RRMSE = 52%, N = 20) whereas over more turbid coastal area (Pärnu Bay) and in lakes the ratio 560/709 worked much better (Fig. 4, Table 3). In general, all tested band ratio algorithms tended to overestimate low Z_{SD} values (<3 m), but this was less pronounced with the ratio 560/709 (Fig. 4a).

The retrieval of Secchi depth via $K_d(490)$ increased the accuracy (Figs. 3, 4, Table 3) in comparison to the band ratio algorithms. All models showed similar validation statistics independently of the conversion factors used. The most accurate results (Fig. 4b) were

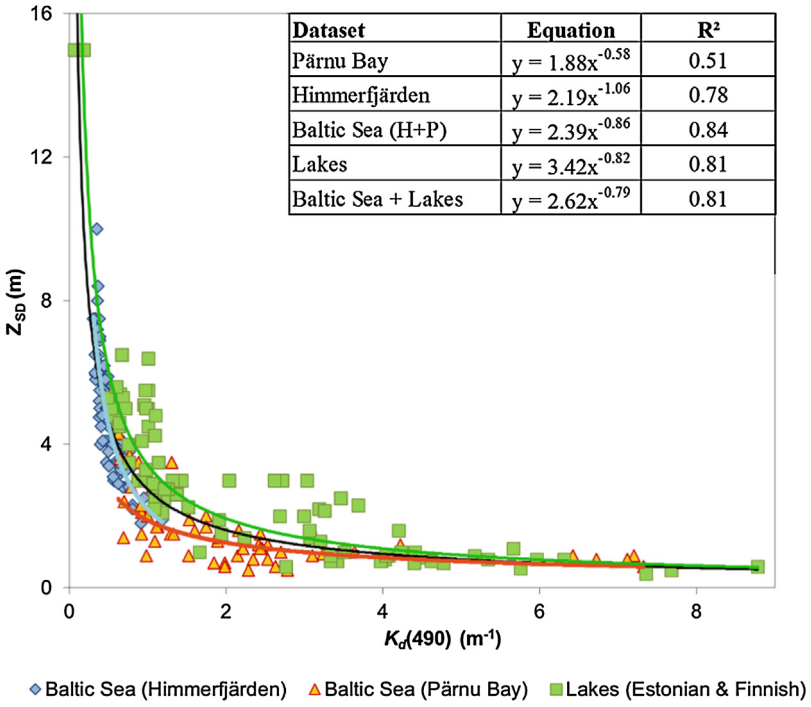

Fig. 2. Relationship between Secchi depth and $K_d(490)$ for two coastal areas in the Baltic Sea and for lakes from the SUVI dataset both on a regional scale and also as merged data over regions.

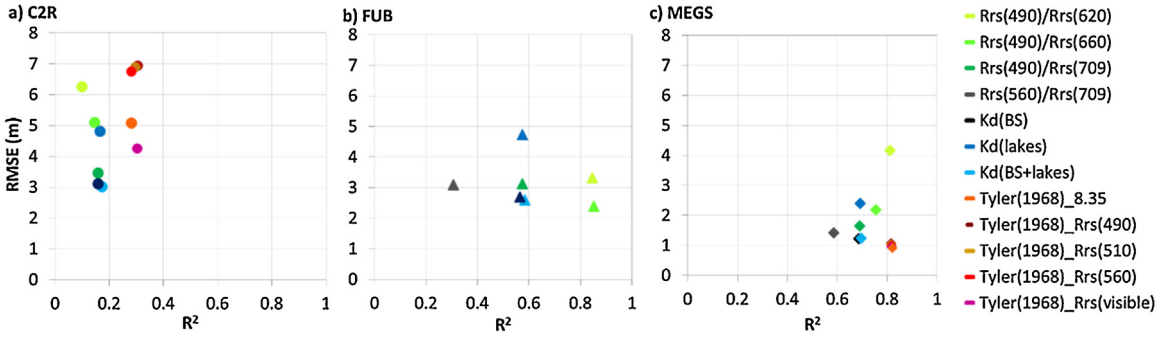

Fig. 3. The coefficient of determination (x-axis) and respective root mean square errors (y-axis) over coastal validation sites for all models retrieving Z_{SD}. The model predictions have been estimated for flagged pixels based on three different processors (a) C2R, (b) FUB, (c) MEGS.

Table 3
Comparison of validation results (R^2, RMSE, n) of three main methods (560/709 band ratio, $K_d(490)$ and Z_{sd} conversion factors based on Baltic Sea and Lakes dataset and via $R_{rs}(560)/K_d(\lambda)+c(\lambda)$ in Baltic Sea (Himmerfjärden, Pärnu Bay) and lakes (Vättern, Vänern, Mälaren, Võrtsjärv, Peipsi). The symbol $\sum$ denotes that summary statistics have been calculated over all areas. The results are based on the flagged data.

	$560/709K_d(\lambda)K_d(\lambda)+c(\lambda)$			$560/709K_d(\lambda)K_d(\lambda)+c(\lambda)$			$560/709K_d(\lambda)K_d(\lambda)+c(\lambda)$		
	R^2			RMSE (m)			n		
Vättern							1	1	1
Vänern	0.64	0.24	0.78	1.64	1.51	0.95	10	10	10
Mälaren	0.75	0.66	0.90	0.46	0.50	0.56	35	35	35
Võrtsjärv	0.25	0.56	0.91	0.66	0.29	0.20	8	4	4
Peipsi	0.21	0.77	0.70	0.63	0.50	0.59	10	9	9
Pärnu Bay	0.47	0.47	0.49	1.24	1.00	0.95	11	11	11
Himmerfjärden	0.00	0.00	0.64	1.94	1.99	0.99	19	19	19
$\sum$	0.68	0.75	0.91	1.98	1.33	0.77	94	89	89

retrieved with the conversion factors based on the Baltic Sea and Lakes datasets ($Z_{SD} = 2.62^{*}K_d(490)\hat{} - 0.79$).

The use of the theoretical relationship between $K_d(\lambda)+c(\lambda)$ and Secchi depth yielded the most accurate validation results (Table 3, Fig. 4). The statistics were rather similar in case of all three approaches (Fig. 4c–e) used to calculate the coupling constant in Eq. (3). With the use of a predefined coupling constant (8.35), the values of the Z_{SD} were underestimated in more transparent waters, indicating a single constant is not suitable for all water types. Similar results were obtained by the use of a single band (either at 490, 510, 560 nm) in the coupling constant – while the band 560 nm (Fig. 4d) gave most accurate results and best alignment around 1:1

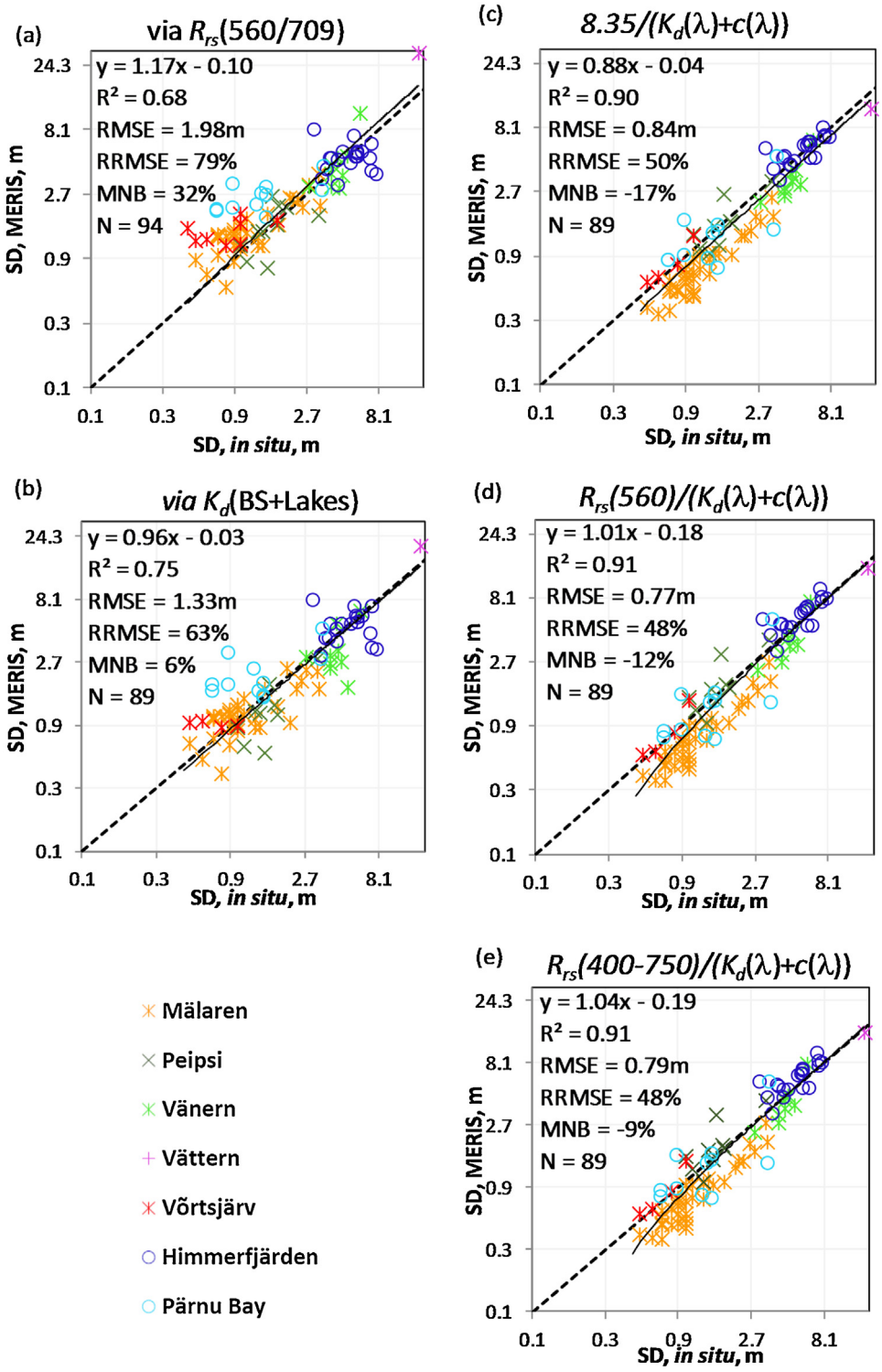

Fig. 4. Matchup analysis for the most accurate Z_{SD} retrievals from three main methods: (a) I approach via R_{rs}(560/709); (b) II approach calibrated on the lake and Baltic Sea datasets; (c)–(e) via the underwater visibility theory with various sets of coupling constants c) pre-calculated coefficient 8.35; (d) MERIS R_{rs} at 560 nm; e) all MERIS R_{rs} values over the region 400–750 nm weighted with the sensitivity of the human eye. The results are based on the MEGS flagged data.

line (intercept = 1.01, slope = 0.18) over all water bodies considered together, it still slightly underestimated the value of Z_{SD} in the very clear, oligotrophic Lake Vättern (in situ Z_{SD} 14.8 m, model 13.5 m) which was better estimated by using the band at 490 nm (model Z_{SD} estimated 14.4 m). In that sense, the use of the whole reflectance spectrum in the visible to calculate the coupling constant (Fig. 4e) seems to be more robust for different types of water. In general the approach to calculate the coupling constant for each match-up pixel separately (either by using single band or the whole spectrum) showed the highest accuracy (R^2 = 0.91, RMSE = 0.77m, n = 89).

3.3. Example of transparency product over the baltic sea and nordic lakes

The Secchi depth algorithm was applied on MERIS full resolution L2 images and monthly means from March to September in

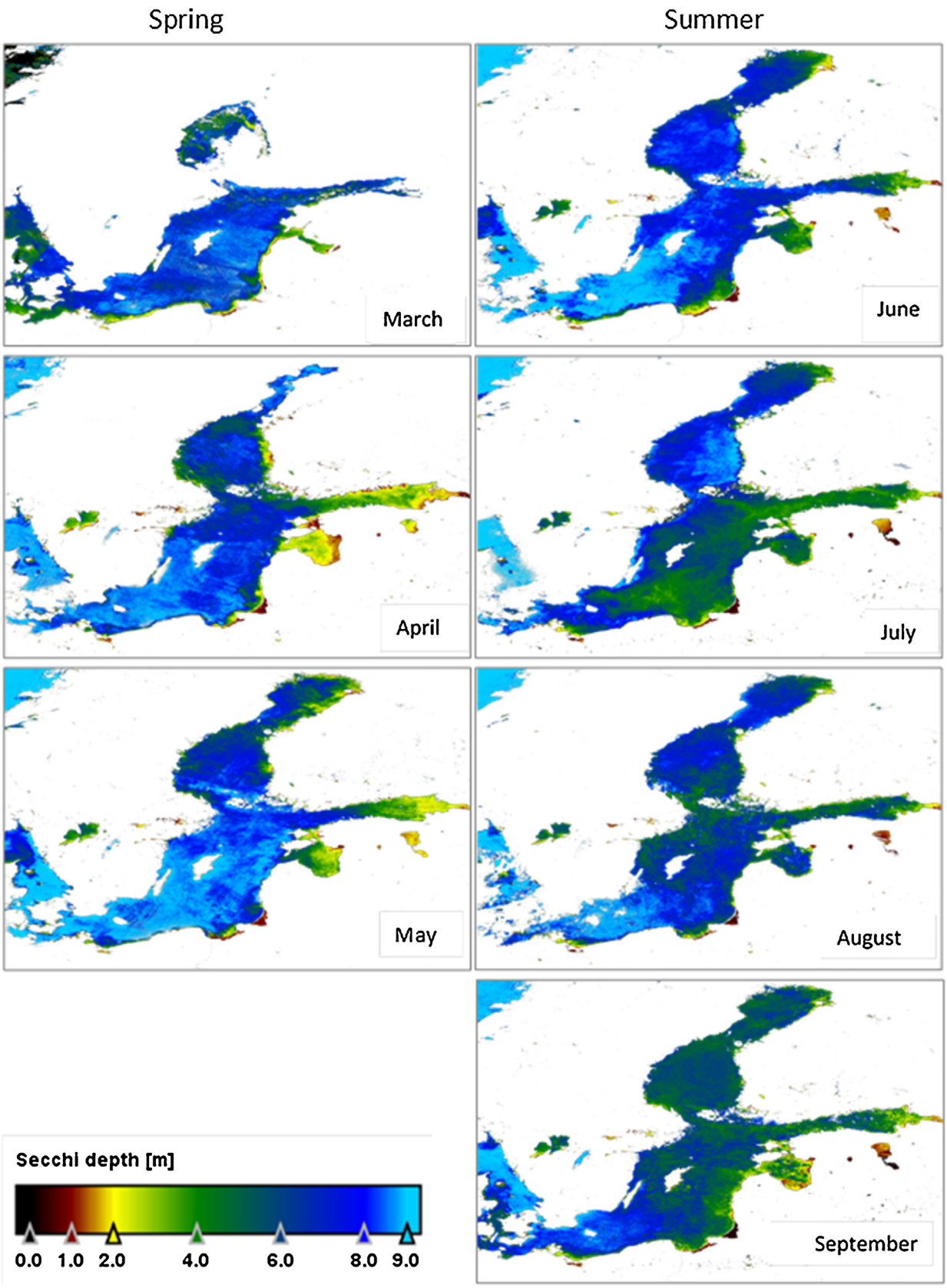

Fig. 5. Monthly means of Secchi depth algorithm (8.35, $K_d(\lambda)+c(\lambda)$, flag ice_haze) for 2010.

2010 were calculated (Fig. 5). Year 2010 was selected because of the suitable conditions (cloudless weather during MERIS overpasses) to retrieve good and spatially homogeneous transparency estimates.

Over the Baltic Sea, ice cover was present in Gulf of Bothnia in March and April which refer to lower transparency in the spring months compared to the summer months. Possibly, the spring bloom devel-

opment may have been triggered by the ice melt in April. Monthly means also illustrate the effect of big river inflows (Kokemaenjoki in the eastern part of the Bothnian Sea, the river Neva in the eastern Gulf of Finland, the river Daugava in the Gulf of Riga, and the rivers Nemunas and Vistula in the south-eastern part of the Baltic proper and the river Oder in the SW Baltic) on the transparency which was most pronounced in April, indicating the input of nutrients to the Baltic Sea due to snow melt. Independently from the month, less transparent waters tend to be present by the eastern coast of the Baltic Sea: Vistula (Gulf of Gdansk), Curonian Lagoon, Arkona Basin, Pärnu Bay (Gulf of Riga). In the closed area of the eastern part of Gulf of Finland, the effect of the river input from the Neva is evident over all months, nutrient loaded waters increase the amount of TSM and Chl a in the water and thus decrease the transparency. Additionally, the effect of cyanobacterial blooms onto the water transparency is visible in the center of the Baltic Sea (Northern Baltic proper, Western Gotland Basin, Eastern Gotland Basin, Bornholm Basin) in July and in the Gulf of Bothnia in August and September.

Over the large Nordic lakes, ice cover was present in March and April. Fig. 5 shows that the algorithm describes well the heterogeneous spatial distribution of water transparency over Lake Vänern (more turbid coastal areas) and Lake Mälaren (east-west trend in water transparency) in Sweden and in Lake Peipsi (north-south trend in water transparency) in Estonia. Additionally, the lower transparency in the lakes during the summer months due to cyanobacterial blooms is also visible in Lake Peipsi and in Lake Võrtsjärv.

The intensity and extent of highly dynamic coastal processes and seasonal dynamics inside lakes could therefore be well described using remote sensing data. Depending on the cloud cover and satellite overpass it would allow to map water transparency on a daily basis and also level 3 composites over longer periods of time could be calculated, e.g. by using monthly composite images. The systematically acquired, spatially and temporally frequent remote sensing data could thus be used as an additional source of information for assessment and WFD and MSFD reporting purposes.

4. Discussion

The aim of this study was to test and develop appropriate optical methods that can be applied for estimating water transparency, and to evaluate the reliability of the derived products. Using various algorithms, MERIS-derived Z_{SD} values were tested against in situ data measured in Baltic Sea coastal waters and in large Northern European lakes. The results demonstrated that water transparency can be retrieved with high accuracy and good resolution by the means of ocean color remote sensing (300 m resolution), and also resolve the Secchi depth in coastal bays and inland waters.

Secchi Depth values were derived by three different approaches a) via band ratio algorithms; b) via $K_d(490)$; and c) via the theoretical relationship between $K_d(\lambda)+c(\lambda)$ and Z_{SD}. The large variety of validation sites with large ranges of optical properties (e.g. most transparent L.Vättern $8.5 < Z_{SD} < 16.2$ m compared to L.Võrtsjärv $0.2 < Z_{SD} < 2.6$ m) allowed to estimate the algorithm performance on lake and water type basis.

4.1. Underwater visibility theory

The application of underwater visibility theory (Tyler, 1968; Preisendorfer, 1986) for deriving Z_{SD} from MERIS data resulted in the highest accuracy ($R^2 = 0.91$, RMSE = 0.77 m, RRMSE = 48%, n = 89) over all areas. The results were well aligned around the 1:1 line and no systematic errors could be found. Overall this method described well the Secchi depth from oligotrophic to eutrophic conditions. According to the approach used for calculating the coupling constant in the underwater visibility theory, there were only rather minor differences in the validation results.

The application of underwater visibility theory gave most accurate results when the MERIS reflectance at 560 nm was used in the numerator for calculating the coupling constant for each match-up pixel between satellite and in situ data separately. Although based on only one match-up where the Secchi depth was >10 m, the results indicated that for more transparent waters reflectance at 490 nm would give more accurate results, which still needs to be verified using a more extensive match-up dataset. The good results using 490 nm for more transparent waters may be explained by the lower amount of absorbing and scattering substances in clearer waters where the light penetration maximum is at 490 nm. This maximum is shifted towards the red part of the spectrum (i.e. longer wavelengths) in the case of more turbid waters, i.e. inland and coastal waters.

The use of all MERIS bands in the visible spectrum to calculate the coupling constant showed more robust results, but with similar accuracy. This gave also a good fit around the 1:1 line and was suitable for all water types, although the slope and intercept ($y = 1.04x + 0.19$, $R^2 = 0.91$) were slightly better in case of using $R_{rs}(560)$ ($y = 1.01x + 0.18$, $R^2 = 0.91$). The good performance of this method can be explained that despite using the whole spectrum in the visible domain, it has been also related to the photopic sensitivity of the human eye which has maximum at 555 nm, half-peak values at 510 and 610 nm and 1% of the maximum at 438 and 687 nm (Aas et al., 2014). Therefore, the bands at 510, 560 and 620 nm had the highest weights and these are also the bands which have shown the highest accuracy when validated with in situ data over optically-complex waters (Kratzer and Vinterhav, 2010).

Many studies (Tyler, 1968; Holmes, 1970; Kallio, 2006; Aas et al., 2014 and references therein) have shown that there is no universal relationship between $K_d(\lambda)+c(\lambda)$ and Z_{SD} in the underwater visibility theory and the use of a pre-defined coupling constant has its limitation in case of different water types as shown in this study as well. Additionally, the underwater visibility theory relies on the good retrieval of the $K_d(\lambda)$ and especially $c(\lambda)$ which is in general higher than $K_d(\lambda)$ in the visible domain. Although the validation of $K_d(490)$ algorithm has shown high accuracy (RMSE 13%, MNB 1.1%, Alikas et al., 2015a) when compared to in situ data, the retrieval of $c(\lambda)$ has not been validated yet. In order to apply Lee et al. (2015) modified underwater visibility theory, good remote sensing algorithms to derive spectral $K_d(\lambda)$ at specific wavelengths are required.

4.2. Accuracy of satellite-based water quality products

Poor performance of the products of FUB and C2R in comparison with MEGS can be explained by the accuracy of the $R_{rs}(\lambda)$ product. Kratzer and Vinterhav (2010) have shown that over optically-complex waters, the $R_{rs}(\lambda)$ is retrieved more accurately by the MEGS atmospheric correction in comparison to FUB and C2R (*e.g* for the ICOL pre-processed images, over the coastal station the accuracy (RMSE) of the $R_{rs}(560)$ by MEGS (9.1%), FUB (23.9%) and C2R (37.3%)).

Independently of the approach used, the Z_{SD} algorithm validation resulted in highest errors and lowest correlation coefficient in the case of Himmerfjärden bay where most of the in situ data used to validate the algorithms originated from summer 2008. An exceptional bloom of the prymnesiophyte *Chrysochromulina* spp. was observed at that time over the whole Baltic Sea (Kratzer and Vinterhav, 2010). This rather rare event in turn created complex conditions for the atmospheric correction and the reflectance retrieval by MEGS, leading to higher uncertainties, which in turn propagates errors to the Z_{SD} product.

4.3. Uncertainties in secchi depth measurements

Additionally the uncertainties (RMSE = 0.78 m, RRMSE = 48%, R^2 = 0.91, N = 89 in best case) in deriving Z_{SD} from remote sensing data could be partly explained by the in situ data used for the validation. These can vary depending on the size of the Secchi disk and also with the person taking the measurements due to the properties of the human eye as a contrast sensor. While there is little difference between taking Z_{SD} measurements on the sunlit or shadow side of the boat, Aas et al. (2014) estimated it to be on average 7% lower on the shadow side of the ship. Furthermore, the accuracy of Z_{SD} reading depends also on wind speed with an estimated error in the range of 0.2–0.5 m (depending on wind speed), as wind-induced waves and ship drifting make it difficult to estimate the exact depth below the waves. Additionally, Mikaelsen and Aas (1990) showed that taking the Z_{SD} measurements with a 30 cm disk using a water telescope increased the values by about 11% on average. Also, the satellite-derived Z_{SD} originates from an area around 300 × 300 m, indicating a clear difference in scale of observation. This may have a very strong effect, especially in patchy algal bloom conditions.

4.4. Satellite data for environmental monitoring and reporting

Remote sensing provides systematic and synoptic measurements with high temporal and spatial coverage. The achievements of the past 20 years have led to the recognition of remote sensing data as a source of information for monitoring purposes. We demonstrated here that Z_{SD} is reliable measure of water transparency from space. Due to the advances in technology using MERIS the method can be used both in coastal and inland waters reliably. Secchi depth is generally used as an indicator for eutrophication in the Baltic Sea by HELCOM (2007) and is also considered as important ecological parameter in the EU WF and MSF Directives which have stressed the need to monitor water transparency.

The potential of including remote sensing data into environmental assessment has been analysed and recommended (Chen et al., 2004, 2007b; Harvey et al., 2015) and measures to derive numeric water quality criteria from various EO sensors have been proposed (Schaeffer et al., 2011, 2013). Fleming-Lehtinen et al. (2015) concluded that inclusion of remote sensing data into assessment would increase the confidence due to better data availability. Although it has been highlighted that the transferability and repeatability of remote sensing methods can be a challenge (Politi et al., 2012), various studies have shown that remote sensing data provides a great complement to in situ data to map variety of parameters e.g. Chl *a* (Bresciani et al., 2011, 2012); phycocyanin absorption (Gómez et al., 2011); phytoplankton biomass and transparency (Alikas et al., 2015b); cover and distribution of aquatic vegetation (Hunter et al., 2010; Szilágyi 2012); lake habitats (Rowan et al., 2006).

Therefore the data and analyses, now possible through the Europe's Copernicus program and the wide constellation of dedicated environmental monitoring satellites, the Sentinels, have the potential to provide efficient, high confidence and cost effective environmental monitoring capabilities which in combination of past sensors (e.g. MERIS) can provide long term series both backwards and forward in time.

5. Conclusions

The validation of the Secchi depth algorithm showed that while the Z_{SD} algorithm based on the ratio 490/709 was more suitable for relatively clear coastal Baltic Sea waters (i.e. Swedish coastal waters – Himmerfjärden), the ratio 560/709 was more suitable over more turbid coastal (Pärnu Bay) and inland waters. By means of the previously calculated $K_d(490)$ product and by applying region-specific conversion factors, the accuracy of the Secchi depth retrievals increased compared to band ratio algorithm and resulted in smaller RMSE (1.33 m), while describing 75% of the variance in the data. However, both methods (band ratio and K_d) overestimated low and high (Lake Vättern Z_{SD} ~15 m) Z_{SD} values and resulted in some outliers. The use of underwater visibility theory described well the Secchi depth from oligotrophic to eutrophic conditions with high accuracy (R^2 = 0.91, RMSE = 0.77 m, n = 89). The results were well aligned around the 1:1 line (y = 1.01x + 0.18) and no systematic errors were present. Water transparency is considered to be one of the important quality elements to assign the ecological status of the waterbody by the WFD and MSFD. Additionally according to HELCOM (2007) water clarity reflects eutrophication. Therefore monitoring water clarity is required in many international, national and regional agreements, directives, and in the resulting management plans which aim to protect waterbodies in order to assure the sustainable management of these ecosystems. However due to the temporal and spatial variability and inaccessibility of the aquatic environments, the fulfillment of expected monitoring requirements is an acknowledged problem. The use of the remote sensing based Secchi depth product would enhance both the spatial and temporal coverage of the monitoring possibilities, and could be an additional source of information to estimate anthropogenic pressure and the status of aquatic environments.

Acknowledgements

We acknowledge ESA and ACRI-ST for developing ODESA (http://earth.eo.esa.int/odesa). The EU FP7 PEOPLE project WaterS (251527) funded our study and mobility between researchers. Thanks also to Stockholm University's Strategic Research Marine Environment Programme (Baltic Ecosystem Adaptive Management, BEAM) and ESA, contract ESA/ARGANS 4000111320/14/I-LG. We appreciate the comments by three anonymous reviewers who helped to improve this manuscript.

References

Aas, E., Høkedal, J., Sørensen, K., 2014. Secchi depth in the Oslofjord-Skagerrak area: theory, experiments and relationships to other quantities. Ocean Sci. 10, 177–199.

Alikas, K., Kratzer, S., Reinart, A., Kauer, T., Paavel, B., 2015a. Robust remote sensing algorithms to derive diffuse attenuation coefficient for optically-complex waters. Limnol. Oceanogr. Methods 13, 402–415.

Alikas, K., Kangro, K., Randoja, R., Philipson, P., Asuküll, E., Pisek, J., Reinart, A., 2015b. Satellite based products for monitoring optically complex inland waters in support of EU Water Framework Directive. Int. J. Remote Sens. 36, 4446–4468.

Arst, H., Erm, A., Herlevi, A., Kutser, T., Leppäranta, M., Reinart, A., Virta, J., 2008. Optical properties of Boreaal lake waters in Finland and Estonia. Boreal Environ. Res. 13, 133–158.

Austin, R.W., Petzold, T.J., 1981. The determination of the diffuse attenuation coefficient of sea water using the Coastal Zone Color Scanner. In: Garver, J.F.R. (Ed.), Oceanography from Space. Springer, New York, pp. 239–256.

Bourg, L., D'Alba, L., Colagrande, P., 2008. MERIS Smile Effect Characterization and Correction. Technical Note. Retrieved November 21, 2015, from http://earth.eo.esa.int/pcs/envisat/meris/documentation/MERIS_Smile_Effect.pdf.

Bresciani, M., Stroppiana, D., Odermatt, D., Morabito, G., Giardino, C., 2011. Assessing remotely sensed chlorophyll-A for the implementation of the water framework directive in European Perialpine lakes. Sci. Total Environ. 409, 3083–3091.

Bresciani, M., Vascellari, M., Giardino, C., Matta, E., 2012. Remote sensing supports the definition of the water quality status of lake omodeo (Italy). Euro. J. Remote Sens. 45, 349–360.

Chen, Q., Zhang, Y., Ekroos, A., Hallikainen, M., 2004. The role of remote sensing technology in the EU water framework directive (WFD). Environ. Sci. Policy 7, 267–276.

Chen, Z., Muller-Karger, F., Hu, C., 2007a. Remote sensing of water clarity in Tampa Bay. Remote Sens. Environ. 109, 249–259.

Chen, Q., Zhang, Y., Hallikainen, M., 2007b. Water quality monitoring using remote sensing in support of the EU water framework directive (WFD): a case study in the gulf of Finland. Environ. Monit. Assess. 124, 157–166.

Davies-Colley, R.J., Vant, W.N., 1988. Estimation of optical properties of water from Secchi disk depths. Water Resour. Bull. 24, 1329–1335.
Doerffer, R. and Schiller, H. 2008. MERIS regional coastal and lake case 2 water project – atmospheric correction ATBD, GKSS Research Center. Retrieved Janurary 06, 2016, from http://www.brockmann-consult.de/beam-wiki/download/attachments/1900548/meris_c2r_atbd_atmo_20080609_2.pdf.
Doron, M., Babin, M., Mangin, A., Hembise, O., 2007. Estimation of light penetration, and horizontal and vertical visibility in oceanic and coastal waters from surface reflectance. J. Geophys. Res. 112, C06003.
Doron, M., Babin, M., Hembise, O., Mangin, A., Garnesson, P., 2011. Ocean transparency from space: validation of algorithms using MERIS, MODIS and SeaWiFS data. Remote Sens. Environ. 115, 2986–3001.
ESA, 2011. Reference Model for MERIS Level 2 Processing. Third MERIS reprocessing: Ocean Branch. Issue 5.0. Doc. no: PO-TN-MEL-GS-0026-Ocean.
European Commission, 2000. Directive 2000/60/EC of the European Parliament and of the Council of 23 October 2000 establishing a framework for community action in the field of water policy. Offic. J. Eur. Commun. L327 (1. 22.12. 2000).
European Commission, 2008. Directive 2008/56/EC of the European Parliament and of the Council of 17 June 2008 establishing a framework for community action in the field of marine environmental policy (marine strategy framework directive). Offic. J. Eur. Commun. L164 (19 25.06.2008).
Fleming-Lehtinen, V., Andersen, J.H., Łysiak-Pastuszak, E., Murray, C., Pyhälä, M., Laamanen, M., 2015. Recent developments in assessment methodology reveal that the Baltic Sea eutrophication problem is expanding. Ecol. Indic. 48, 380–388.
Gómez, J.A., Alonso, C.A., García, A.A., 2011. Remote sensing as a tool for monitoring water quality parameters for Mediterranean lakes of European Union water framework directive (WFD) and as a system of surveillance of cyanobacterial harmful algae blooms (Scyanohabs). Environ. Monit. Assess. 181, 317–334.
Håkanson, L., Gyllenhammar, A., Brolin, A., 2004. A dynamic compartment model to predict sedimentation and suspended particulate matter in coastal areas. Ecol. Modell. 175, 353–384.
HELCOM, 2007. Baltic sea action plan. In: HELCOM Ministerial Meeting, Poland.
Harvey, T., Kratzer, S., Philipson, P., 2015. Satellite-based water quality monitoring for improved spatial and temporal retrieval of chl-a in coastal waters. Remote Sens. Environ. 158, 417–430.
Holmes, R.W., 1970. The Secchi disk in turbid coastal waters. Limnol. Oceanogr. 15, 688–694.
Hunter, P.D., Gilvear, D.J., Tyler, A.N., Willby, N.J., Kelly, A., 2010. Mapping macrophytic vegetation in shallow lakes using the compact airborne spectrographic imager (CASI). Aquat. Conserv. Mar. Freshw. Ecosyst. 20, 717–727.
Kallio, K., 2006. Optical properties of Finnish lakes estimated with simple bio-optical models and water quality monitoring data. Nord. Hydrol. 37, 183–204.
Kirk, J.T.O., 1994. Light and Photosynthesis in Aquatic Ecosystems, 2nd ed. Cambridge University Press.
Kratzer, S., Vinterhav, C., 2010. Improvement of MERIS level 2 products in Baltic Sea coastal areas by applying the Improved Contrast between Ocean and Land processor (ICOL)—data analysis and validation. Oceanologia 52, 211–236.
Kratzer, S., Hakansson, B., Sahlin, C., 2003. Assessing Secchi and photic zone depth in the Baltic Sea from space. AMBIO 32, 577–585.
Kratzer, S., Brockmann, C., Moore, G., 2008. Using MERIS full resolution data (300 m spatial resolution) to monitor coastal waters–a case study from Himmerfjärden, a fjordlike bay in the north-western Baltic Sea. Remote Sens. Environ. 112, 2284–2300.
Kratzer, S., 2000. Bio-optical studies of coastal waters. In: Monograph in English. School of Ocean Sciences, Univ. of Wales (Ph.D. thesis).
Lee, Z.P., Shang, S., Hu, C., Du, K., Weidemann, A., Hou, W., Lin, J., Lin, G., 2015. Secchi disk depth: a new theory and mechanistic model for underwater visibility. Remote Sens. Environ. 169, 139–149.
Mikaelsen, B., Aas, E., 1990. Secchi Disk Depths and Related Quantities in the Oslofjord 1986–87, Report 77. University of Oslo, Oslo.
Mobley, C.D., 1994. Light and Water: Radiative Transfer in Natural Waters. Elsevier, New York.
Mueller, J.L, 2000. SeaWiFS algorithm for the diffuse attenuation coefficient, K (490) using water-leaving radiances at 490 and 555 nm. In SeaWiFS Postlaunch Calibration and Validation Analyses, ed. S. B. Hooker, and E.R Firestone, 24–27. Greenbelt, Maryland.
Paavel, B., Arst, H., Metsamaa, L., Toming, K., Reinart, A., 2011. Optical investigations of CDOM-rich coastal waters in Pärnu Bay. Eston. J. Earth Sci. 60, 102–112.
Politi, E., Cutler, M.E.J., Rowan, J.S., 2012. Using the NOAA advanced very high resolution radiometer to characterise temporal and spatial trends in water temperature of large european lakes. Remote Sens. Environ. 126, 1–11.
Poole, H.H., Atkins, W.R.G., 1929. Photo-electric measurements of submarine illumination through-out the year. J. Mar. Biol. Assoc. U.K. 16, 297–324.
Preisendorfer, R.W., 1986. Secchi disk science: visual optics of natural waters. Limnol. Oceanogr. 31, 909–926.
Rowan, J.S., Carwardine, J., Duck, R.W., Bragg, O.M., Black, A.R., Cutler, M.E.J., Soutar, I., Boon, P.J., 2006. Development of a technique for lake habitat survey (LHS) with applications for the european union water framework directive. Aquat. Conserv. Mar. Freshw. Ecosyst. 16, 637–657.
Santer, R., Zagolski, F., 2008. ICOL.Improve Contrast Between Ocean & Land. ATBD – MERIS Level-1C. Université du Littoral Côte d'Opale, Wimereux – France.
Schaeffer, B.A., Hagy, J.D., Conmy, R.N., Lehrter, J.C., Stumpf, R.P., 2011. An approach to developing numeric water quality criteria for coastal waters using the SeaWiFS satellite data record. Environ. Sci. Technol. 46, 916–922.
Schaeffer, B.A., Hagy, J.D., Stumpf, R.P., 2013. Approach to developing numeric water quality criteria for coastal waters: transition from SeaWiFS to MODIS and MERIS satellites. J. Appl. Remote Sens. 7 (073544-18).
Schroeder, T., Schaale, M., Fischer, J., 2007. Retrieval of atmospheric and oceanic properties from MERIS measurements: a new Case-2 water processor for BEAM. Int. J. Remote Sens. 28, 5627–5632.
Szilágyi, F., 2012. Remote sensing of aquatic vegetation to comply with the needs of the water framework directive. Israel J. Plant Sci. 60, 135–150.
Tyler, J.E., 1968. The Secchi disc. Limnol. Oceanogr. 13, 1–6.
Vant, W.N., Davies-Colley, R.J., 1984. Factors affecting clarity of New Zealand lakes. N. Z. J. Mar. Freshw. Res. 18, 367–377.
Vertucci, F.A., Likens, G.E., 1989. Spectral reflectance and water quality of Adirondack mountain region lakes. Limnol. Oceanogr. 34, 1656–1672.
Wang, M., Son, S., Harding, Jr., L.W., 2009. Retrieval of diffuse attenuation coefficient in the Chesapeake Bay and turbid ocean regions for satellite ocean color applications. J. Geophys. Res. 114, C10011.